Dipole scattering in highly polar semiconductor alloys

Wei Zhao and Debdeep Jena
Department of Electrical Engineering, University of Notre Dame, Notre Dame, Indiana 46556

(Received 2 March 2004; accepted 11 May 2004)

The wide gap polar semiconductors III-V nitrides, II-VI oxides, and ferroelectrics exhibit large spontaneous and piezoelectric polarization due to their nonsymmetric crystal structures. Electrical conductivity in alloys of such crystals is degraded by scattering from the varying polarization coupled to alloy disorder. We have modeled this effect by dipole scattering. We have calculated dipole scattering limited mobility in the relaxation time approximation of the Boltzmann equation. The results are applied to $Al_xGa_{1-x}N$ layers coherently strained on GaN. For a typical carrier concentration of 10^{18} (cm^{-3}) in $Al_{0.3}Ga_{0.7}N$, dipole scattering limited mobilities are 2535 and 3420 ($cm^2/V\ s$) at 300 and 77 K, respectively. Applying our results to ferroelectric alloys, we reach the interesting conclusion that dipole scattering in such alloys will lead to extremely low mobilities (1–10 $cm^2/V\ s$), since it degrades as the square of average dipole moment. This leads us to suggest that digital alloy growth might be necessary to achieve high conductivities in highly polar wide gap alloy semiconductors and ferroelectrics for device applications. © *2004 American Institute of Physics*. [DOI: 10.1063/1.1767615]

I. INTRODUCTION

Dipole scattering is an important phenomenon in electromagnetic theory; the color of the sky is believed to be due to dipole scattering of light wave by molecules in the atmosphere. Such scattering of electron waves in solids is a much less explored phenomenon. Dipole scattering in highly compensated semiconductors such as Si, Ge, and GaAs had been studied a long time ago by Stratton,[1] Boardman,[2] Ridley[3] to account for the scattering of carriers by ionized donor and acceptor pairs. The form of dipole scattering presented in this work originates due to fundamentally different origin—due to the material inhomogeneity, *even in the absence of any impurities*. It is well known that the III-V nitride[4–7] and II-VI oxide[8] semiconductors (GaN/InN/Aln and ZnO/CdO/MgO families), as well as ferroelectric semiconductors[9,10] ($LiNbO_3$ and $BaTio_3$) exhibit strong electronic polarization because of their nonsymmetric crystal structures and large bond ionicity. Carriers moving in alloys composed of these highly polar materials will experience scattering due to the spatially varying polarization coupled with the alloy disorder. In this work, we study the effect of this polarization disorder on the electrical conductivity in such alloys by showing that the carrier scattering is a form of dipole scattering.

The effect of dipole scattering on the mobility of a quantum-confined two-dimensional electron gas at the AlGaN/GaN interface due to the varying dipole moment in $Al_xGa_{1-x}N$ barrier was recently investigated.[6] In that work, the conductivity of mobile electrons spatially separated from the dipoles in the barrier layer resulted in a weak degradation of conductivity due to remote dipole scattering. However, dipole scattering for carriers physically located *in the polar alloys* has not been studied yet. Highly polar semiconductor alloys, most notably AlGaN and InGaN have found applications in various optical and electronic devices. Such alloys form the active layers of light emitting diodes and LASERs,[11,12] high-power and high speed field-effect transistors such as the novel polarization-doped field effect Transistor,[13] base regions of heterojunction bipolar transistors (HBTs),[14] and active layers of solar-blind photodetector.[15] So it is important to understand the basic transport properties of carriers in these polar alloys to find the fundamental limits placed by compositional disorder.

In this paper, we derive the dipole-scattering-limited mobility in the relaxation time approximation of Boltzmann transport equation employing a virtual crystal approximation for disorder of dipole moment. We apply our results to the case of carriers moving in coherently strained $Al_xGa_{1-x}N$ layer on GaN. The dependence of dipole- scattering mobility on alloy ratio (Al content in $Al_xGa_{1-x}N$), carrier concentration, and temperature is investigated. We compare the strength of dipole scattering with that due to alloy disorder scattering and phonons (acoustic and optical) for different carrier concentration and temperatures. We find dipole scattering is stronger than alloy scattering for very low carrier density and low temperature. Our result is general and it can be used for analyzing transport in other interesting highly polar materials such as oxide and ferroelectrics alloys. By applying our results to the very highly polar ferroelectric semiconductor alloys, we find that dipole-scattering limits the mobility to extremely low values, and point out strategies to deal with this problem for improving the conductivity.

II. THEORY

A. Scattering dipole moment *P* and density of scattering sites

If the dipole moment in every unit cell was the same, there would be no scattering of electrons since the dipole potential would then be periodic. Translational symmetry of the dipole potential is broken in random alloys, the effect of which is best captured by a virtual crystal approximation (VCA).[6] The average scattering dipole moment P for the

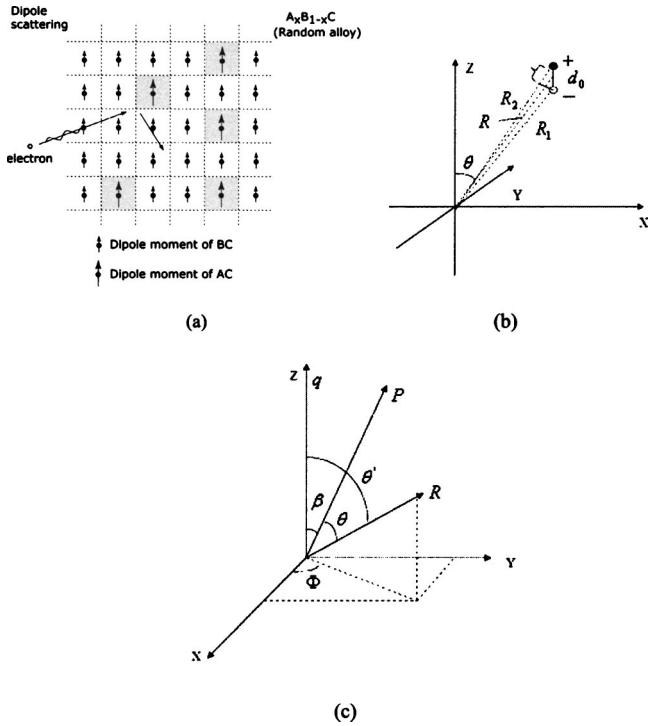

FIG. 1. (a) shows the dipole distribution in the diluted $Al_xGa_{1-x}N$ alloy. Al sites have larger dipole moment than Ga sites. (b) denotes the relative location of dipoles with respect to electron at the origin, where R_1 and R_2 are the distance of negative and positive charge from the origin, d_0 is the distance between the two opposite charges in the dipole, R is the distance between the dipole center origin. (c) is the coordinate system for Fourier transformation. P is the dipole moment and it is on the y-z plane. $q=k_2-k_1$ is the wave vector and R is the real space vector.

alloy $A_xB_{1-x}C$ at *each site* is given by

$$P = ed_0 = 2x(1-x)|\Delta P|,$$

$$\Delta P = P_1(x) - P_2(x), \tag{1}$$

where x is the alloy ratio, $P_1(x)$ and $P_2(x)$ are the dipole moments (including spontaneous. and piezoelectric polarization if the alloy is strained) per unit cell for alloy components 1 (*AC*) and 2 (*BC*), respectively. The scattering potential thus derived differs from alloy scattering potential, which is typically taken to be the conduction band discontinuity (for electrons) between the two binary semiconductors forming the alloy, or experimentally determined alloy-scattering parameter.[7] The density of dipoles n_0 is just the density of unit cells, since according to the VCA, dipole moment in *every cell* deviates from the spatially averaged moment. Thus $n_0=1/v_0$, where v_0 is the volume of a unit cell of the alloy semiconductor.

B. Derivation of dipole-scattering mobility

The distribution of dipoles is shown in Fig. 1(a) for the alloy $A_xB_{1-x}C$, whose components AC and BC have different polarizations. Carriers experience dipole scattering due to the randomness of dipole moment. The relative location between the dipole and the electrons is in Fig. 1(b). The unscreened Coulomb potential at the origin is given by

$$V_{\mathrm{UNS}}(R,\theta) = \frac{e^2}{4\pi\varepsilon_s}\left[\frac{1}{R_1} - \frac{1}{R_2}\right] \approx \frac{eP\cos(\theta)}{4\pi\varepsilon_s R^2}, \tag{2}$$

where P is the dipole moment defined as $P=ed_0$ (d_0 is the distance between the two opposite charges in a dipole), $\varepsilon_s=\varepsilon_r\varepsilon_0$ is the (static) dielectric constant, and θ is the angle between R and P.

To apply Fermi's Golden Rule for the scattering rate from plane wave such as electron wave vector state $|k\rangle \rightarrow |k+q\rangle$, we use the Born approximation to get the scattering matrix element. We evaluate the Fourier transformation of this potential in the wave vector (q) space, where we choose z axis along the q direction and P in the y-z plane, as shown in Fig. 1(c). Using the relation $\cos(\theta)=\cos(\beta)\cos(\theta')+\sin(\theta')\sin(\Phi)\sin(\beta)$ we get

$$V_{\mathrm{UNS}}(q) = \int V_{\mathrm{UNS}}(R,\theta)e^{iq^*R}d^3R = \frac{ep}{\varepsilon q}\cos(\beta), \tag{3}$$

where β and θ are the angles between q and P, q and R, respectively.

We also directly get the screened potential for the dipole scattering

$$V_{\mathrm{SC}}(R,\theta) = \frac{e^2}{4\pi\varepsilon_s}\left[\frac{e^{-R_1/L_D}}{R_1} - \frac{e^{-R_2/L_D}}{R_2}\right] \approx \frac{e}{4\pi\varepsilon_s}\frac{P\cos(\theta)}{R^2}\left(1+\frac{R}{L_D}\right)e^{-R/L_D} \tag{4}$$

by using the approximation: $y_2-y_1 \approx (x_2-x_1)dy/dx = \Delta x dy/dx$. L_D is the Debye screening length. Here we assume $d_0 \ll L_D$. Then we use Fourier transformation to get the screened potential in the wave vector space

$$V_{\mathrm{SC}}(q) = \int V_{\mathrm{SC}}(R,\theta)e^{iq\cdot R}d^3R = \frac{V_{\mathrm{UNS}}(q)}{\varepsilon(q)}, \tag{5}$$

where $q_D=1/L_D$ is the Debye-Huckel wave vector, and $\varepsilon(q)=1+q_D^2/q^2$ captures the effect of screening. The momentum scattering rate is calculated from the relaxation time approximation of the Boltzmann equation as

$$\frac{1}{\tau_m(k)} = n_0\frac{\hbar k}{m^*}\frac{2\pi P^2\cos^2(\beta)}{(L_D k^2 a_0)^2 e^2}\left[4k^2L_D^2 - 2\ln(1+4k^2L_D^2) + \frac{4k^2L_D^2}{1+4k^2L_D^2}\right], \tag{6}$$

where $m^*=m_rm_0$ is the electron effective mass (m_0 being the electron rest mass), $a_0[=4\pi\varepsilon_s/m^*e^2=0.53(\varepsilon_r/m_r)\ \text{Å}]$ is the effective Bohr radius, n_0 is the dipole concentration, and k is the electron wave vector. Angular averaging over random orientations of electron momenta yields $\langle\cos^2(\beta)\rangle=1/2$.

The total momentum scattering time is found by the averaging procedure for a Fermi-Dirac distribution

$$\langle \tau_m \rangle = \frac{2}{3} T \frac{\int_0^\infty dE[AE' - 2\ln(1+AE') + AE'(1+AE')^{-1}]E^3 \exp(E'-E_F)[1+\exp(E'-E_F)]^{-2}}{\int_0^\infty dE' \sqrt{E'}[1+\exp(E'-E_F)]^{-1}}, \tag{7}$$

where $T = 8\sqrt{\pi}(N_C/n_0)(L_D/d_0)^2(m^* a_0^2/\hbar)$ is a time constant characteristic of dipole scattering, and $A = 8m^* L_D^2 k_B T/\hbar^2$ is a dimensionless factor. E' and E_F, carrier energy and Fermi energy, are normalized by the thermal energy $k_B T$. The denominator in Eq. (7) is a Fermi-Dirac integral of order 1/2. To arrive at the average momentum scattering time, a numerical evaluation of Eq. (7) is required, and the resultant mobility is derived from the Drude relation

$$\mu = \frac{e\langle \tau_m \rangle}{m^*}. \tag{8}$$

However, to gain insight into the transport physics, it is instructive to consider the nondegenerate and degenerate limits of carrier concentrations for which approximate analytical forms for mobility can be expected. For analyzing these extreme degeneracy conditions, we define the Fermi energy and the screening lengths used for our calculations clearly.

C. Fermi energy and Debye screening length

Dipole-scattering-limited mobility is strongly dependent on the Fermi energy (E_F) and the Debye screening length (L_D). We use the Pade approximation[16] to get E_F for a given carrier concentration

$$E_F \approx \ln\left(\frac{N}{N_C}\right) + A_1\left(\frac{N}{N_C}\right) + \left[K_1 \log\left[1 + K_2\left(\frac{N}{N_C}\right)\right] - K_1 K_2\left(\frac{N}{N_2}\right)\right] \quad E_F < 15 k_B T, \tag{9}$$

$$E_F \approx \left(\frac{3\sqrt{\pi}N}{4N_C}\right)^{2/3} \quad E_F \geqslant 15 k_B T, \tag{10}$$

where $K_1 = 4.7$, $K_2 = 0.0459$, $A_1 = 0.3535$, and the Pade approximation is valid for small $E_F < 15 k_B T$. Equation (10) is the inverse first-order Sommerfeld approximation, valid for $E_F > 15 k_B T$.

The Debye length is given in the most general case[17] by

$$L_D = \sqrt{\frac{\varepsilon_s k_B T}{e^2 N_C F_{-1/2}(E_F)}}, \tag{11}$$

where $F_{-1/2}(E_F)$ is the Fermi-Dirac integral of order $-1/2$.

D. Nondegenerate and deep degenerate limits

For extreme degeneracy, the dipole-scattering-limited mobility may be derived by using the following approximations. Momentum relaxation time in Eq. (7) can be cast into the form

$$\tau_m(k) = \tau_0 \left(\frac{E}{k_B T}\right)^2, \tag{12}$$

where τ_0 does not depend on carrier energy, and is given by $\tau_0 = (\sqrt{\pi}\hbar/k_B T)(a_0/d_0)^2(N_C/n_0)$. So the mobility for strongly nongenerate carriers can be approximated using the Maxwell-Boltzmann statistics as[18]

$$\mu \approx \frac{8}{3}\left(\frac{\hbar}{k_B T}\right)\left(\frac{e}{m^*}\right)\left(\frac{a_0}{d_0}\right)^2\left(\frac{N_C}{n_0}\right). \tag{13}$$

and we immediately note that $\mu \propto T^{1/2}(m^*)^{3/2} n_0^{-1}$. We note that the dependence of mobility on temperature, effective mass, and dipole density is similar to that calculated by Stratton.[1] For heavily degenerate carrier concentrations, the carrier energy is approximated by Fermi energy, and we can get from Eq. (7)

$$\tau \propto \frac{k n_0^{-1}}{\left[1 - \frac{2\ln(1+4k^2 L_D^2)}{4k^2 L_D^2} + \frac{1}{1+4k^2 L_D^2}\right]}. \tag{14}$$

Near absolute zero temperature, $k^2 L_D^2$ is got from the deep-degeneracy approximation[19]

$$k^2 L_D^2 = (\sqrt[3]{3N\pi^2})^2 \left(\sqrt{\frac{2\varepsilon_S E_F}{3e^2 N}}\right)^2 = \left(\frac{N}{N_0}\right)^{1/3}, \qquad N_0 = \frac{64}{3\pi^5 a_0^3} = 4.64 \times 10^{23}\left(\frac{m_r}{\varepsilon_r}\right)^3 (\mathrm{cm}^3), \tag{15}$$

where N is the carrier density and N_0 is a critical density defined by the effective Bohr radius a_0 of the semiconductor. For very large $k^2 L_D^2$ (due to small effective mass or large dielectric constant and high carrier concentration), it is straightforward to show that $\mu_{\mathrm{dipole}} \propto N^{1/3}$ consistent with Stratton's result.[1] However, for a highly polar alloy, for example, $Al_{0.3}GaN_{0.7}N$ with $m^* = 0.26 m_0$ and $\varepsilon_r = 9$, we get $N_0 = 1.12 \times 10^{19}$ (cm^{-3}). If the carrier density N is very low, i.e., $N \leqslant 10^{14}$ cm^{-3} while it is still in the deep degeneracy region for extremely low temperature (around 0 K, we can see $\mu_{\mathrm{dipole}} \propto n_0^{-1} N^{-1/3}$. For practical carrier concentrations ($N \leqslant 10^{20}$ cm^{-3}) in the semiconductor, $k^2 L_D^2$ is in the order of 0.1–1 and there is no simple carrier concentration dependence for dipole-scattering mobility. The calculated dipole-scattering mobility first decreases and then increases with N at very low temperature (in the highly generate region), i.e., the dependence is not monotonic [as seen in Fig. 6(a)]. This is attributed to the competing effects of screening, carrier kinetic energy, and available final states for scattering.[2]

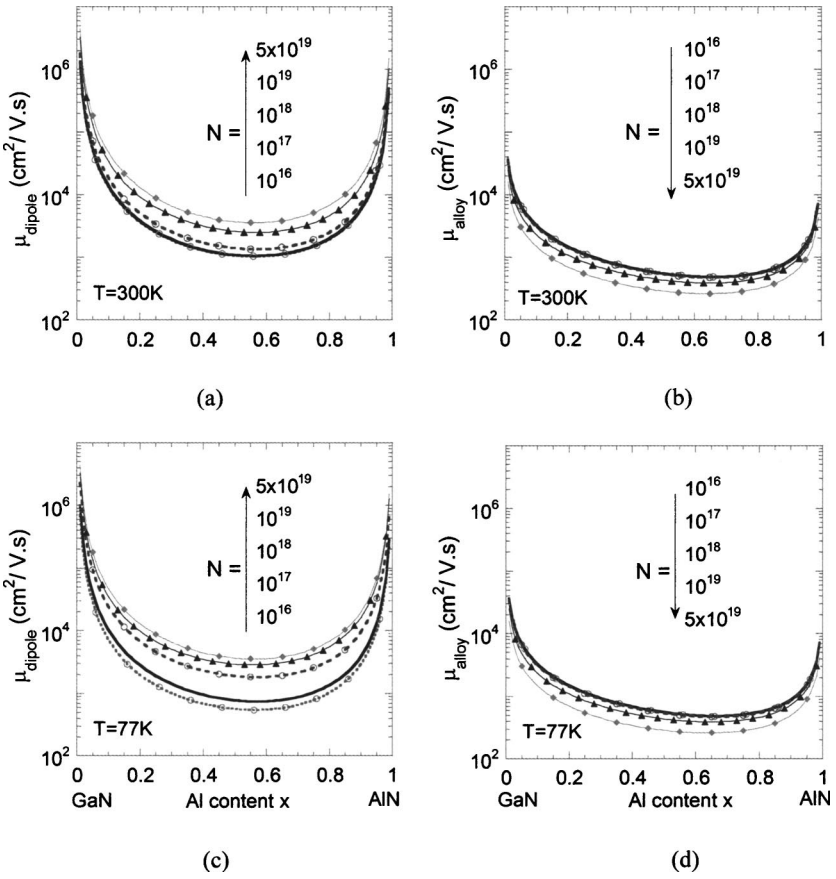

FIG. 2. (a) and (b) are the calculated dipole (μ_{dipole}) and alloy-scattering mobility (μ_{alloy}) vs Al composition in coherently strained $Al_xGa_{1-x}N$ on GaN for different carrier concentrations N at $T=300$ K; (c) and (d) are the same at $T=77$ K. The carrier concentrations are in unit of cm^{-3}.

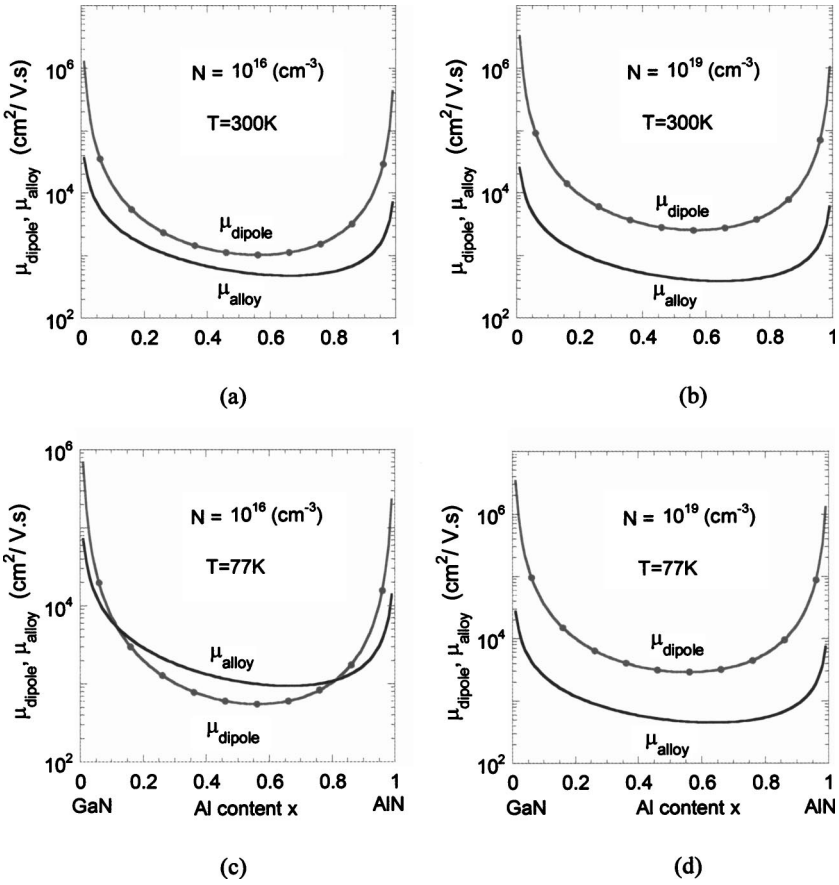

FIG. 3. Comparison of alloy-and dipole-scattering mobility μ_{dipole} vs Al content in $Al_xGa_{1-x}N$ at $T=300$ K (a) (b) and $T\approx 77$ K (c) (1). The carrier concentration $N=10^{16}$ (a), (c) and $N=10^{19}$ cm^{-3} (b) (d) are used for comparison.

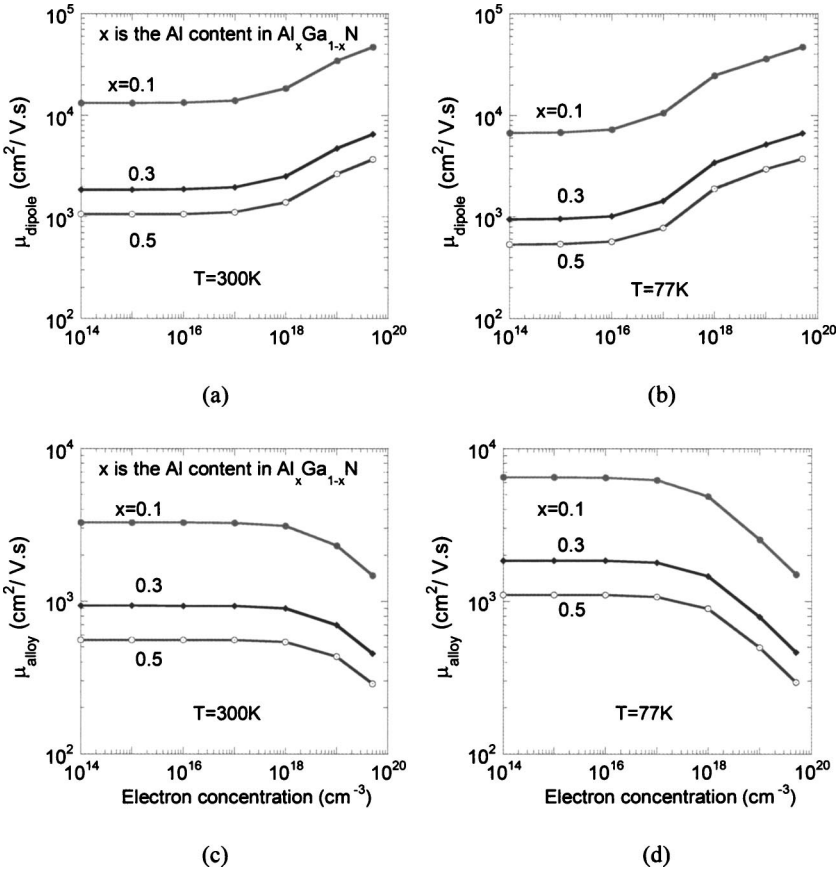

FIG. 4. (a) and (b) are dipole-scattering mobility μ_{dipole} vs electron concentration with different Al composition at $T=300$ K and $T=77$ K, respectively. (c) and (d) are the same for alloy-scattering-limited mobility μ_{alloy}.

E. Calculation of alloy scattering

Dipole scattering is coupled with alloy scattering due to the compositional disorder of the alloy. So it is instructive to compare both alloy-scattering-and dipole-scattering-limited mobility for different alloy compositions, and determine which mechanism dominates. Alloy-scattering-limited mobility is given by[20]

$$\mu_{\text{alloy}} = \frac{2e\hbar}{3\pi m^* V_0^2 \Omega x(1-x)} \frac{k_B T}{n} \ln(1 + e^{E_F/k_B T}), \tag{16}$$

where Ω is the x-dependent volume of unit cell over which the alloy-scattering potential V_0 is effective. E_F is the normalized Fermi energy.

III. APPLICATION TO CARRIER TRANSPORT IN COHERENTLY STRAINED AlGaN ON GaN

At high temperatures, polar optical phonon scattering is usually the dominant scattering mechanism. The effects of other mechanisms such as dipole-scattering, ionized impurity, and alloy-scattering dominate transport properties at lower temperatures. We have calculated the dipole-scattering-limited electron mobility for $Al_xGa_{1-x}N$ pseudomorphically grown on relaxed GaN with varying electron densities. Here we assume the electrons are not from conventional impurity doping; instead they come from polarization doping,[21] photon excitation (such as the generated e-h pairs in the intrinsic AlGaN layer of p-i-n photodioded,[15] or by electrical injection in the base of a heterojunction bipolar

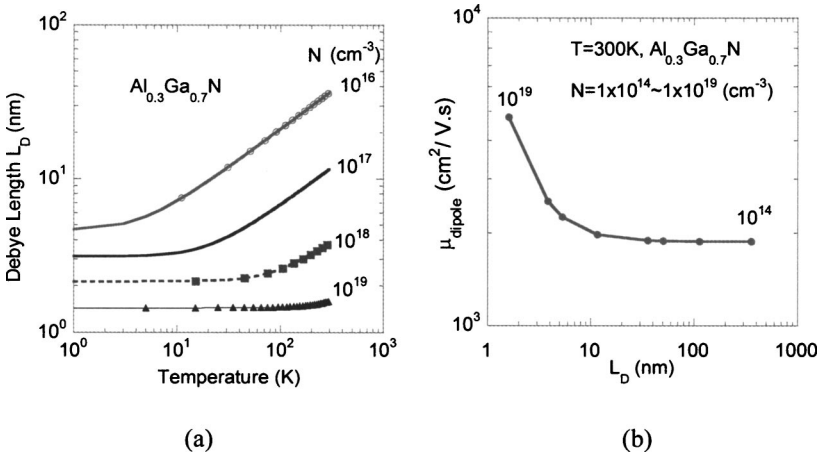

FIG. 5. (a) Deby length L_D as a function of temperature for different carrie concentrations. (b) Calculated dipole-scattering mobility μ_{dipol} vs Debye length L_D at $T=300$ K, $N=10^{14} \sim 10^{19}$ cm^3, and $x=0.3$ in $Al_xGa_{1-x}N$.

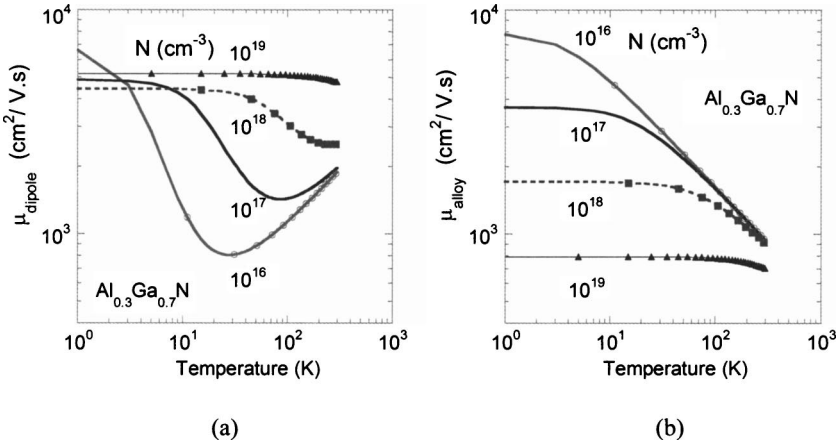

FIG. 6. (a) and (b) Dipole-(μ_{dipole}) and alloy-scattering mobility (μ_{alloy}) vs temperature for different electron concentrations N, respectively.

transistors HBTs.[14] Carriers resulting from impurity doping tend to have a much lower mobility due to ionized impurity scattering. Figure 2 shows the dipole-(a), (c) and alloy-(b), (d) scattering limited mobility for different Al contents (x) for different carrier densities at $T=300$ K (a), (b) and $T=77$ K (c), (d). For dipole-scattering mobility versus x, we can see the expected U shape because the magnitude of average scattering, dipole moment at each site is proportional to $x(1\text{-}x)$. Dipole-scattering-limited mobility *increases* with carrier concentration; the trend is opposite for alloy scattering. It is true for both $T=300$ and 77 K. We have chosen the alloy-scattering potential to be close to the conduction band discontinuity, determined experimentally by magnetoresistance measurements $V_0=1.8$ eV for $Al_xGa_{1-x}N$.

At room temperature alloy scattering is dominant over dipole scattering for both high (10^{19} cm^{-3}) and low (10^{16} cm^{-3}) carrier concentrations for any alloy ratio x [Figs. 3(a) and 3(b)]. However, dipole scattering begins to be dominant for low carrier densities at $T=77$ K over a wide range of x [Fig. 3(c)]. In Fig. 4, we show the dipole-and alloy-scattering limited mobility as a function of electron concentration with different Al ratios at both $T=300$ and 77 K. The dipole-scattering-limited mobility increases monotonically with carrier concentration, due to better screening. But at low carrier concentrations, the dipole-scattering mobility is almost independent of carrier concentration, which means dipole scattering will have a weak dependence on Debye screening length L_D when it is long. This argument is verified in Fig. 5(b), where dipole scattering mobility is plotted as a function of the Debye length L_D, while other parameters are kept constant. Debye length is varied by changing the carrier concentration N from 10^{14} to 10^{19} cm^{-3}. The saturation behavior is clear. In deep degeneracy, only those carriers near Fermi energy will contribute to the dipole scattering. The higher carrier concentration leads to better screening and higher Fermi energy both of which will reduce dipole scattering.

For alloy-scattering limited mobility, the dependence of mobility on the carrier concentration is just the opposite to that of dipole scattering. This occurs due to the short-range nature of alloy scattering, where screening does not play a role.

We investigate the dependence of dipole [Fig. 6(a)] and alloy [Fig. 6(b)] scattering mobility on temperature for different carrier concentrations N. At very low temperatures ($T\leqslant 10$ K), normal carrier density will bring the alloy into extremely high degeneracy (to be almost metallic for $N=10^{19}$ cm^{-3} at $T\leqslant 10$ K), which makes dipole-scattering-limited mobility *independent* of temperature since L_D does not vary with T (Fig. 5(c)]. At higher temperatures, dipole-scattering-limited mobility first decreases to a valley and then increases due to the competing effects of L_D and carrier energy.[2] The valley position roughly corresponds to the temperature at which the alloy switches from degenerate to nondegenerate region. We note that dipole-scattering-limited mobility is not a monotonic function of carrier density N at temperature near 1 K. Figure 7 zooms into the mobility of Fig. 6(a) at 1 K and shows the mobility for different carrier concentrations N. This seemingly strange phenomenon has been referred to in Sec. II D. Here we have to take into account the three competing effects of carrier energy, L_D and available scattering states on dipole-scattering mobility. For low N (but still in highly degenerate region at 1 K), the carrier energy (or Fermi energy) is also low and the available states for scattering are less. This is different from Stratton's result,[1] who predicts $\mu_{dipole}\propto N^{1/3}$ in degenerate region for dipole scattering in a highly compensated semiconductor. Alloy scattering is a short-range event and its mobility correlates closely with the available density of states for scattering. So mobility limited by alloy scattering *decreases* with temperature.

The calculated total mobility versus temperature for

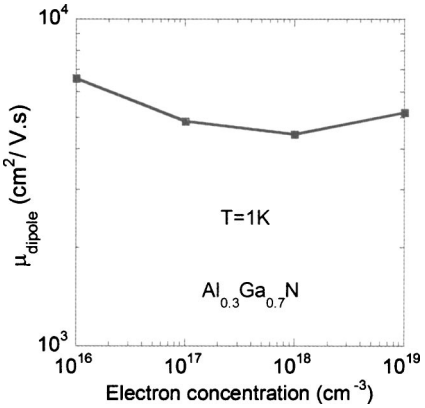

FIG. 7. Dipole-scattering-limited mobility μ_{dipole} as a function of carrier concentration N at $T=1$ K, $x=0.3$ in $Al_xGa_{1-x}N$.

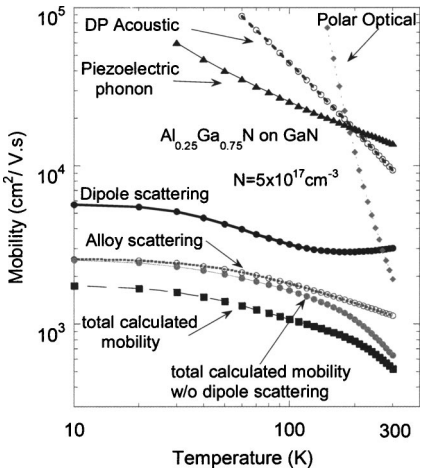

FIG. 8. Calculated total mobility vs temperature considering all contributing scattering mechanisms for electrons ($N=5\times10^{17}$ cm^{-3}) in the coherently strained $Al_{0.25}Ga_{0.75}N$ on GaN.

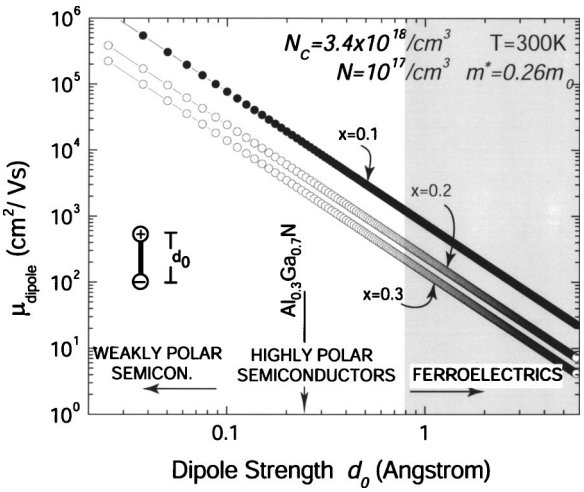

FIG. 9. Dipole-scattering mobility μ_{dipole} for different alloy composition as a function of the dipole strength d_0 per unit cell. Note that ferroelectric semiconductors are expected to have very strong dipole scattering, and the conductivity will be low in such alloys.

electrons ($N=5\times10^{17}$ cm^{-3}) in coherently strained $Al_{0.25}Ga_{0.75}N$ on GaN is shown in Fig. 8 along with all contributing scattering mechanisms. Here we neglect impurity scattering and electrons are created *without* impurity doping, as mentioned before. We can see that alloy scattering is dominant over others for the particular case of AlGaN, but dipole scattering still plays a non-negligible role throughout the whole temperature range. Also shown in Fig. 8 is the calculated total mobility without considering dipole scattering and a large difference is evident between it and the total mobility (calculated by including dipole scattering).

Although we present calculations for dipole scattering in $Al_xGa_{1-x}N$, it is easy to predict the mobility limits set by dipole scattering for other highly polar materials such as II-VI oxides and ferroelectric semiconductors. Figure 9 shows the mobility dependence on the dipole strength d_0 (the distance between positive and negative charge) per unit cell ($d_0=\Delta P/e$) for three different alloy ratios. From Eq. (7), we can see that mobility decreases as the *square* of the polarization in the material, i.e., $\mu_{\text{dipole}}\sim(\Delta P)^{-2}$. Carrier concentration, temperature, electron effective mass, and N_C are assumed to be 10^{17} cm^{-3} 300 K, $0.26m_0$, and 3.4×10^{18} cm^{-3}, respectively. The point corresponding to dipole-scattering mobility of $Al_{0.3}Ga_{0.7}N$ is also marked in Fig. 9. So, we predict that ferroelectric alloys with high ΔP will exhibit an undesirably low dipole-scattering-dominated mobility [$\mu_{\text{dipole}}\sim1-10$ cm^2 (V/s)]. This leads us to suggest digital alloy growth in order to reduce the randomness of dipoles and to reduce the effect of dipole scattering on the carrier mobility, which is important for achieving high conductivity layers in device structures based on these materials.

IV. CONCLUSION

In this work, we have presented a comprehensive analysis of the effect of dipole scattering in highly polar semiconducting and ferroelectric alloys. Dipole scattering rates were derived from relaxation time approximation of the Boltzmann transport equation. We found expressions for dipole-scattering-limited electron mobility for nondegenerate and deep-degenerate limits. The results were applied to study electron conductivity in coherently strained $Al_xGa_{1-x}N$ alloy on GaN. We investigated the dependence of dipole-scattering-limited mobility on carrier concentration, temperature, and alloy compositions. In nondegenerate region, the mobility increases monotonically with both temperature and carrier concentration; however, we found no simple dependence of dipole-scattering-limited mobility on carrier concentration for deep degeneracy. We have also compared the relative strengths of alloy scattering and dipole for the particular case of AlGaN. Based on our theoretical results, we expect a very low dipole-scattering-limited mobility for alloys with large polarization, and suggest digital alloy growth in order to improve the carrier conductivity. Our results are most useful for the devices that utilize highly polar wide band gap III-V nitride and II-VI oxide semiconductors, and many other *ferroelectric* semiconductor alloys that have gained importance lately.

[1]R. Stratton, J. Phys. Chem. Solids **23**, 1011 (1962).
[2]A. D. Boardman, Proc. Phys. Soc. Jpn. **85**, 141 (1965).
[3]B. K. Ridley, *Quantum Process in Semiconductors* (Clanderon, Oxford, 1982), p. 168.
[4]O. Ambacher *et al*., J. Appl. Phys. **87**, 334 (2000).
[5]F. Bernardini and V. Fiorentini, Phys. Status Solidi B **216**, 391 (1999).
[6]D. Jena, A. C. Gossard, and U. K. Mishra, J. Appl. Phys. **88**, 4724 (2000).
[7]D. Jena *et al*., Phys. Rev. B **67**, 153306 (2003).
[8]E. archive New Semiconductor Materials Characteristics and Properties http://www.ioffe.rssi.ru/SVA/NSM
[9]W. A. Doolittle, G. Namkoong, A. G. Carver, and A. S. Brown, Solid-State Electron. **47**, 2143 (2003).
[10]V. M. Fridkin, *Ferroelectric Semiconductors* (Consultant's Bureau, New York, 1980).
[11]S. Nakamura *et al*., Appl. Phys. Lett. **70**, 1417 (1997).
[12]H. Sakai, T. Takeuchi, S. Sota, M. Katsuragawa, M. Komori, H. Amano, and I. Akasaki, J. Cryst. Growth **189/190**, 831 (1998).
[13]Debdeep Jena, Ph.D thesis, University of California, 2003, p. 122.
[14]P. M. Asbeck *et al*., Solid-State Electron. **44**, 211 (2000).
[15]E. J. Tarsa *et al*., Appl. Phys. Lett. **77**, 316 (2000).
[16]L. A. Coldren and S. W. Corzine, *Diode lasers and Photonic Integrated Circuits* (Wiley, New York, 1995), p. 417.
[17]Debdeep Jena, Ph.D. thesis, University of California, 2003, p. 146.
[18]Debdeep Jena, Ph.D. thesis, University of California, 2003, p. 118.
[19]K. Seeger, *Semiconductor Physics–An Introduction* (Springer, Berlin 1985), p. 118.
[20]C. Hamaguchi, *Basic Semiconductor Physics* (Springer, Berlin, 2001).
[21]D. Jena *et al*., Appl. Phys. Lett. **81**, 4395 (2002).